Estimates of the critical exponents of single-crystal $La_{0.73}Ba_{0.27}MnO_3$

Wei Li, H. P. Kunkel, X. Z. Zhou, and Gwyn Williams
Department of Physics and Astronomy, University of Manitoba, Winnipeg, Manitoba, Canada R3T 2N2

Y. Mukovskii and D. Shulyatev
Moscow State Steel and Alloys Institute, Moscow 119049, Russia

(Received 2 July 2004; revised manuscript received 17 September 2004; published 14 December 2004)

The analysis of detailed magnetization measurements, supplemented by zero-field ac susceptibility data, on single-crystal $La_{0.73}Ba_{0.27}MnO_3$ indicates the occurrence of a continuous ferromagnetic-to-paramagnetic phase transition at 245 K. This transition is characterized by exponent values $\gamma = 1.39(2) \pm 0.005$, $\beta = 0.364 \pm 0.003$, and $\delta = 4.83 \pm 0.04$, and these, along with estimates for the critical amplitudes, suggest that this transition falls into the universality class of the near-neighbor, three-dimensional Heisenberg model. Such a result has been predicted by simulations for double-exchange coupled systems in which anisotropy does not play a major role. Low temperature magnetization data indicate that any effects due to spin canting are minimal.

DOI: 10.1103/PhysRevB.70.214413 PACS number(s): 75.40.Cx, 75.50.Cc, 75.50.Pp, 75.30.Cr

I. INTRODUCTION

Transition metal oxides have been the subject of a wide range of investigations—both experimental and theoretical—for many years. The focus of such studies has more recently become particularly intense in the case of the high T_C cuprates and colossal magnetoresistive (CMR) manganites. These materials share considerable structural similarities, and while members of both classes of materials often display semiconducting behavior at high temperatures, the superconductivity of the cuprates is replaced, typically, by a magnetically ordered ground state in the manganese perovskites. While the high T_C cuprates have been studied for close to two decades, an explanation of this behavior—particularly the fundamental physics as it relates to the mechanism yielding such elevated transition temperatures—remains controversial. CMR behavior in the manganese perovskites, by contrast, was first reported[1] over half a century ago, but despite these earlier studies and the revival of interest[2] in this phenomenon due to its more recent "rediscovery," the underlying physical mechanism is, likewise, the subject of ongoing debate. In both classes of materials, however, the possible role played by (spontaneous) electronic phase separation has emerged as the focus of much discussion.[3,4]

The present paper does not concentrate on this latter issue, *per se*, but on a related, perhaps more specific issue, but one which is equally controversial; specifically, the nature of the magnetic phase transition that is frequently observed in close proximity to the metal-insulator transition (and the attendant CMR) in the doped Mn perovskites (general formula $L_{1-x}A_xMnO_3$, where L is a rare earth, including La, and A a divalent alkaline earth ion). While this paramagnetic-to-ferromagnetic transition can be first order/discontinuous[5] or second order/continuous,[6] what is perplexing is the result that in $La_{1-x}Sr_xMnO_3$ with $x \sim 0.25$ where a consensus exists on the occurrence of a continuous paramagnetic-to-ferromagnetic transition, quite different values for the associated critical exponents have been reported,[7–9] a point returned to in more detail below. Within the broader perspective of the intrinsically inhomogeneous phase separation scenario, it is expected that transitions displaying first order characteristics can be driven toward second order by the effects of disorder.[10] Indeed, in competing theories of CMR based on bipolaron pair breaking effects,[11] both first order and continuous magnetic transitions are possible, with the nature of the magnetic transition reflecting a critical polaron density at the transition temperature. Either of these approaches—as indeed do others[12]—presents a general (rather than a system specific) explanation of the behavior of CMR materials. As a corollary, given the current consensus that the magnetic interactions in these materials are predominantly double exchange and superexchange, then one would certainly expect that the magnetic transitions—the paramagnetic-to-ferromagnetic transition in particular—should be described by the same universality class. This makes the careful estimates of critical exponents describing continuous magnetic transitions in these systems particularly important since *if* such exponents are indeed different, it might indicate some further subtlety in the physics of these materials that has previously been overlooked.

Below we present detailed measurements of the field and temperature dependent magnetization of a bulk single crystal sample (the most appropriate form for the characterization of critical behavior[9]) of $La_{0.73}Ba_{0.27}MnO_3$. Analysis of these data yields exponent values consistent with those predicted for the three-dimensional, near-neighbor Heisenberg model. Available transport data on this system support these conclusions. Specifically, the trend that the magnitude of the (colossal) magnetoresistance near T_C in mixed valence manganites displays not only an inverse dependence on T_C but may also reflect the order of the attendant paramagnetic-to-ferromagnetic phase transition.[2] For example, $La_{1-x}Sr_xMnO_3$ ($0.2 \leqslant x \leqslant 0.5$) exhibits some of the highest T_C's among Mn perovskites[9] and displays, correspondingly, a relatively weak magnetoresistance[13] accompanying a second-order/ continuous magnetic phase transition. By contrast, systems such as $Pr_{1-x}Ca_xMnO_3$ ($0.1 \leqslant x \leqslant 0.3$) undergo a first-order/discontinuous magnetic transition at significantly lower T_C's, with an associated magnetoresistance

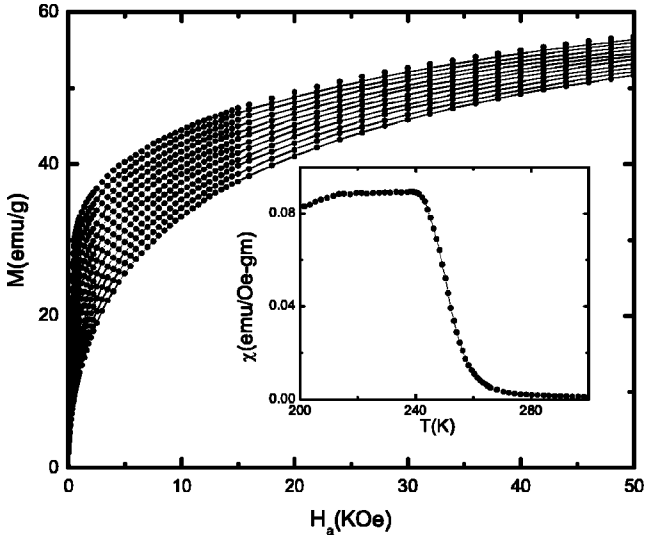

FIG. 1. Magnetization isotherms between 240 and 251 K (in 1 K steps). Inset: the zero-field ac susceptibility (measured on warming).

which is substantially enhanced.[14] In the $La_{1-x}Ba_xMnO_3$ system, transport data on polycrystalline/thin film samples with $x \approx 1/3$ indicate[15] a moderate magnetoresistance (40–50 %), possibly enhanced in polycrystalline materials by grain-boundary effects. It is our intention to check the latter via transport measurements on single crystals. The results of the latter notwithstanding, the previously reported moderate magnetoresistance of this system is consistent with the trends mentioned above and the current conclusions regarding the magnetic response.

II. EXPERIMENTAL DETAILS

The sample used in the present study was a single crystal of mass 0.163 g, a semicylindrical rod of length of 6 mm with an average radius of 1.6 mm. This sample, of nominal composition $La_{0.73}Ba_{0.27}MnO_3$, was grown at the Moscow State Steel and Alloys Institute using the floating zone technique;[16] it was of high quality both structurally—displaying a mosaicity of less than 1°—and magnetically—the coercivity field did not exceed 10 Oe at any temperature below T_C, falling to less than 1 Oe some 10 K below T_c.

Measurements of the dc magnetization in applied fields up to 5 T (oriented along the sample's cylindrical axis) were acquired using a Quantum Design Model PPMS 6000 magnetometer using five-scan averaging. Prior to measuring at any given temperature the sample was demagnetized by warming to 300 K—well above the ordering temperature—and then cooling to a preselected measuring temperature in zero field. At each such temperature a sufficient waiting period was adopted (typically 30 min) to allow the sample to reach thermal equilibrium.

III. RESULTS AND DISCUSSION

A. General features

The inset in Fig. 1 reproduces the temperature dependence of the zero-field susceptibility $\chi(0,T)$ measured at 300 Hz in a 0.1 Oe rms driving field (applied parallel to the cylindrical axis of the sample) on warming between 200 and 300 K following zero-field cooling. There was no discernible hysteresis in this susceptibility within experimental uncertainty (typically 0.1 K). The data in this inset enable two initial but important estimates to be made. From the minimum slope of $d\chi/dT$ one obtains a preliminary value for the ordering temperature of $T_C \approx 248$ K, while the relatively flat region in $\chi(0,T)$ below 240 K—particularly the maximum susceptibility value (identified with N^{-1}) of 0.089 emu/g Oe in this region—provides an estimate of the demagnetizing factor N [=11.2(4)g Oe/emu]. However, even in relatively soft magnetic systems the use of very low ac driving fields means that the maximum measured susceptibility represents a *lower* limit on N^{-1} (i.e., an *upper* limit[17] on N). This appears to be confirmed by calculation;[18] treating the specimen as an ellipsoid with principal axes equal to the listed dimensions—clearly an approximation for the sample used here—and evaluating the corresponding elliptic integral, yields a lower value of $N=9.94$ g Oe/emu (based on a theoretical density of 6.76 g/cm^3).

The main body of Fig. 1 shows a selected series of magnetic isotherms measured in the vicinity of the Curie temperature T_C, estimated above. Such data were collected over the temperature interval 240 to 251 K in 0.5 K intervals, and in 1 K intervals immediately outside this range, using the procedure described in the preceding section.

Before discussing the detailed analysis of these data in the critical regime, some comments of a general nature are appropriate.

First, an obvious point, the magnetization curves in the critical region do *not* display metamagnetic (i.e., S-shaped) characteristics generally associated with a first-order magnetic transition (as has been reported[5] in $La_{1-x}Ca_xMnO_3$ for $x \approx 0.3$). Further evidence that the transition evident in Fig. 1 is of a continuous nature is provided by Arrott-like plots[19] of the type reproduced in the inset in Fig. 2. Here plots of M^2 vs H/M (where $H=H_a-NM$ is the internal field, H_a the applied field, and M the magnetization) show no indication whatsoever of a negative slope [i.e., a term of the form-$a(T)M^4$ in the free energy], particularly in the limit of small H. Such a term has been cited[5] as evidence supporting the presence of a first-order/discontinuous transition in the manganites. It also follows from this inset that conventional Arrott scaling does *not* apply to this sample (these plots do not form a set of parallel straight lines), a result discussed in more detail below. What the isotherms shown in Fig. 1 do reveal is that this system has a technically soft magnetic character (as was also revealed by the zero-field susceptibility approaching the demagnetizing factor limit), with the rapid increase in the magnetization from the $H_a=0$ state being typical of the effects of domain wall motion in soft systems. Close examination of the behavior of these isotherms near T_C also reveals that they approach a shearing curve limited behavior (i.e., approach a maximum slope of N^{-1}). Using data over an applied field range $-50 \leqslant H_a \leqslant 50$ Oe for temperatures at and immediately below $T_C(\sim 10\ \mathrm{K})$ yields a final estimate of $N=10.62$ g Oe/emu, some 5% smaller than that obtained from

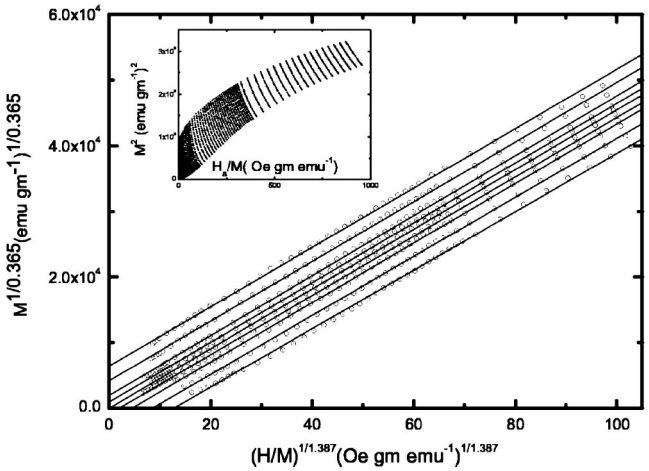

FIG. 2. Modified Arrott plots $[M^{1/\beta}$ vs $(H/M)^{1/\gamma}]$ using Heisenberg model exponents for a selection of magnetic isotherms at temperatures of 242 (top), 243, 244, 244.5, 245, 245.5, 246, 247, and 248 K (bottom). Inset: conventional Arrott plots (M^2 vs H/M) of the magnetization data displayed in Fig. 1.

susceptibility data; this represents good agreement overall considering the nonideal (ellipsoidal) specimen shape.

Finally, from estimates of the saturation moment (86.25 emu/g)—obtained from the 2 K isotherm using an M vs H_a^{-1} plot for data between 6 and 8 T—the Ba composition of this sample is estimated to be $x=0.27(0)\pm0.003$, assuming a spin-only Mn moment. The extent of any spin noncollinearity at 2 K in high applied fields is therefore minimal.

B. Critical behavior

In the immediate vicinity of a second-order phase transition with Curie/ordering temperature T_C, the correlation length ξ diverges according to the power law $\xi(T)=\xi_0(T/T_C-1)^{-\upsilon}$ and the static scaling law equation[20] relates the (reduced) magnetization $m(h,t)$ to the linear scaling fields $t=(T-T_C)/T_C$ and $h\sim H/T_C$, where H is the internal field, via

$$m(h,t)=|t|^{\beta}F_{\pm}\left(\frac{h}{|t|^{\gamma+\beta}}\right). \tag{1}$$

While the general behavior of the scaling function F above (+) and below (−) the transition remains unspecified, its asymptotic behavior for small and large values of its argument leads to the following well established power laws for the spontaneous magnetization $[M_S(T)=M(T,H=0)]$ and its reduced counterpart:

$$M_S(T)=M_S(0)\left(1-\frac{T}{T_C}\right)^{\beta}, \quad m(0,t)\sim B|t|^{\beta} \quad (T<T_C) \tag{2}$$

and the initial susceptibility $[\chi_i(T)=(\partial M/\partial H)_{H=0}]$:

$$\chi_i(T)=\chi_0\left(\frac{T}{T_C}-1\right)^{-\gamma}, \quad \chi_i(t)=\frac{\partial m}{\partial h}\sim Ct^{-\gamma} \quad (T>T_C). \tag{3}$$

Further, at the Curie temperature itself $(T=T_C, t=0)$

$$m(h,0)\sim Dh^{1/\delta} \tag{4}$$

with $\gamma=\beta(\delta-1)$ according to the Widom relation. While the transition temperature T_C can be *estimated* using the approach mentioned above, it and the critical exponents γ,β, and δ have to be determined in a self-consistent manner from detailed analysis of the magnetization data. This analysis usually begins by recognizing that, whereas Eq. (1)–(4) are based on the contribution arising from magnetic critical fluctuations alone (the singular magnetic response), the measured magnetization contains both the singular and additional terms resulting from technical or regular components (i.e., domain wall motion, coherent rotation, etc.). In order to eliminate such technical contributions and complications arising from crystalline anisotropy, the spontaneous magnetization and initial susceptibility appearing in Eq. (2) and (3) are estimated by extrapolation from the "high" field regime (the technically saturated regime) assuming an Arrott-Noakes equation of state[21]

$$\left(\frac{H}{M}\right)^{1/\gamma}=\left(\frac{T-T_C}{T_C}\right)+\left(\frac{M}{M_1}\right)^{1/\beta} \tag{5}$$

where M_1 is a material specific constant. In the above equations H represents the internal field, about which comments are relevant at this point. Three different estimates for the demagnetization factor N have been obtained, as outlined above, and in the calculation of the internal field an average of the two experimentally estimated values has been used. However, given the nonuniform shape of the sample investigated (in spite of which the estimates for N are in relatively good agreement) data for which the demagnetizing field (NM) is a significant fraction of the applied field (H_a) (typically around 50%, or more—essentially for $H_a<350-400$ Oe) have been excluded from this analysis to limit uncertainties from this source.

Modified Arrott plots based on Eq. (5) were made for a range of exponent values $0.9\leqslant\gamma\leqslant1.5, 0.25\leqslant\beta\leqslant0.55$ encompassing the range of extremes between mean-field ($\gamma=1.0, \beta=0.5$) and near-neighbour three-dimensional Heisenberg model predictions[22] ($\gamma=1.396, \beta=0.369, \delta=4.783$). When the appropriate values of γ and β are chosen, isothermal magnetisation (m) vs (internal) field (H) curves form a series of parallel straight lines in such modified plots. To achieve truly self-consistent estimates, however, the intercepts of these straight lines on the vertical and horizontal axes yield $M_S(T)^{1/\beta}$ $(T<T_C)$ and $(1/\chi_i)^{1/\gamma}$ $(T>T_C)$, respectively. Specifically, these straight line extrapolations eliminate the so-called technical contributions, enabling the critical components to be isolated which, in turn, can be (re)tested against the power-law predictions listed above. Self-consistency is achieved when the modified Arrott plots and the ensuing power laws yield the same exponent values. Such power-law tests, of course, require an estimate for T_C to

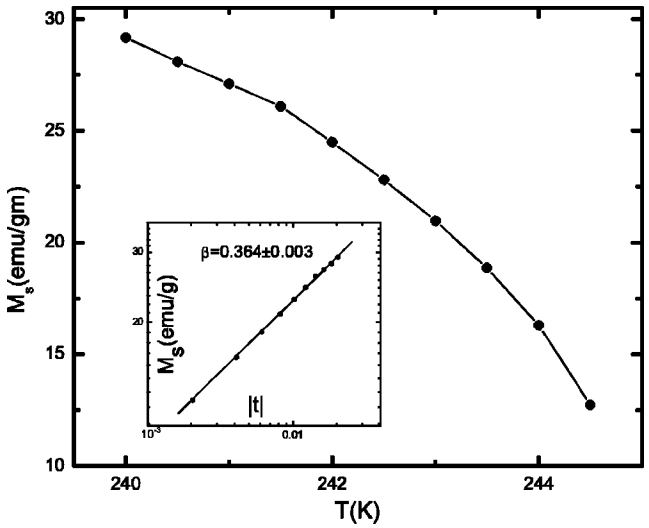

FIG. 3. The spontaneous magnetization M_s (found from the ordinate intercept in Fig. 2) plotted against temperature. The insert reproduces a double logarithmic plot of M_s vs reduced temperature t (using T_C=245 K); the straight line drawn confirms the power-law prediction of Eq. (2) and its slope yields the value for the exponent β shown.

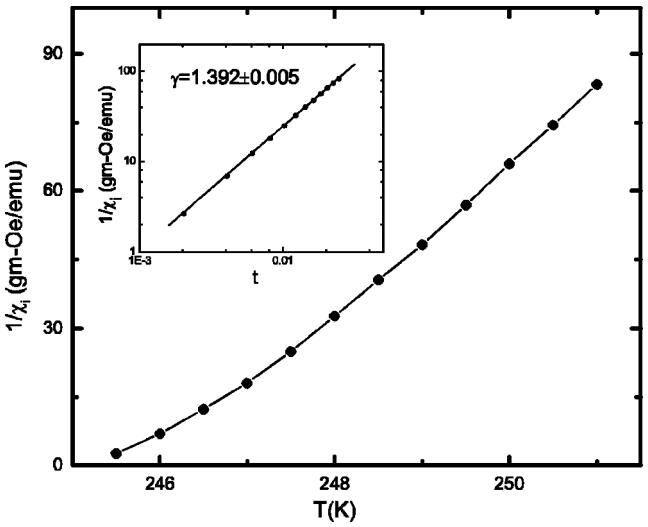

FIG. 4. The initial susceptibility χ_i (found from the abscissa intercept in Fig. 2) plotted against temperature. The inset displays χ_i plotted on a double-logarithmic scale against the reduced temperature t (with T_C=245 K); the straight line drawn confirms the power-law prediction of Eq. (3) and its slope yields the value for the exponent γ shown.

be made, and this is obtained from the isothermal line extrapolating through the origin—the critical isotherm (in practise this usually involves an extrapolation between the temperatures of two or so curves having smallest positive and negative intercepts). Double-logarithmic plots testing Eq. (2) and (3) are then constructed, the slopes of which yield (slightly) modified exponent estimates, and the whole process is iterated until self-consistency is achieved. As detailed below, this is possible for Heisenberg model exponents alone in this system.

The main body of Fig. 2 reproduces modified Arrott plots for data acquired in the range $241 \leqslant T \leqslant 246$ K, $450 \leqslant H_a \leqslant 30\,000$ Oe using Heisenberg model exponents. These data do indeed fall on a set of parallel straight lines and yield an improved estimate of T_C=245 (±0.5) K. By contrast, the inset in Fig. 2 reproduces these data in modified form using mean-field exponents ("conventional" Arrott plots); the significant curvature evident in this inset indicates the inapplicability of such exponents to describe the critical behavior of this single crystal. The self-consistency of Heisenberg exponent estimates is confirmed in Figs. 3 and 4. The first of these figures exhibits the spontaneous magnetization $M_S(T)$ (deduced from the vertical intercepts in Fig. 2) as a function of temperature ($T < T_C$), while the second of these displays the temperature dependence ($T > T_C$) of the inverse initial susceptibility $[\chi_i(T)^{-1}]$ (found from the horizontal intercepts in Fig. 2). The insets in these figures show these same data replotted against the reduced temperature t, using T_C =245.0 K, on a double-logarithmic scale; these insets confirm directly the power-law predictions of Eqs. (2) and (3) and the associated slopes yield

$$\beta = 0.364 \pm 0.003, \quad 2 \times 10^{-3} \leqslant |t| \leqslant 2 \times 10^{-2},$$

$$\gamma = 1.39(2) \pm 0.005, \quad 2 \times 10^{-3} \leqslant t \leqslant 3 \times 10^{-2},$$

both very close to Heisenberg model predictions. With T_C so chosen, Fig. 5 reproduces the field dependence of the magnetization along the critical isotherm; the double-logarithmic plot reproduced in the inset confirming the power-law relationship of Eq. (4) yielding

$$\delta = 4.83 \pm 0.04, \quad 200 \leqslant H \leqslant 50\,000 \text{ Oe},$$

again close to the Heisenberg model value.

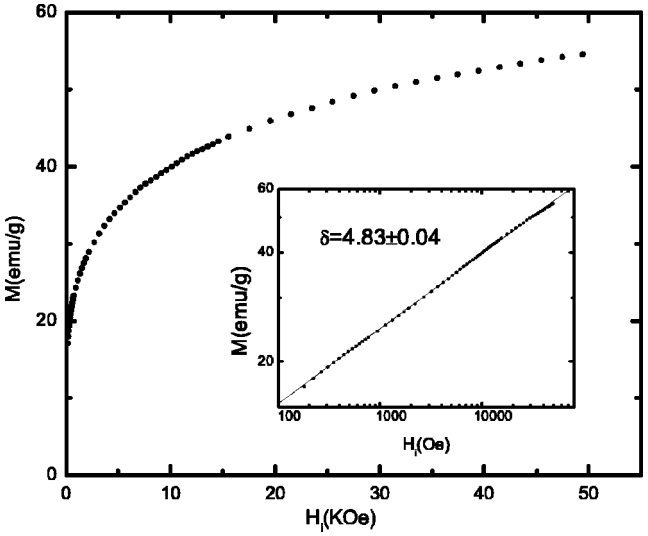

FIG. 5. The critical isotherm—the zero intercept line in Fig. 2 (which gives T_C=245 K). The inset shows these data on a double-logarithmic plot, the straight line nature of which confirms the power-law prediction of Eq. (4); the slope of this line yields the critical exponent value δ shown.

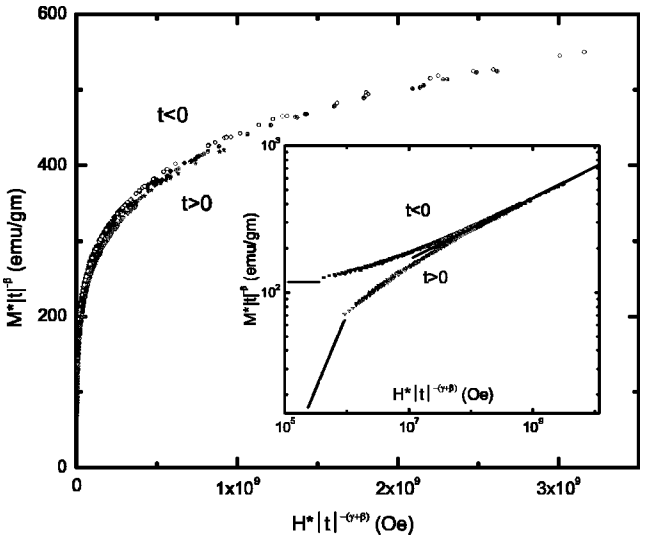

FIG. 6. A scaling plot of M/t^{β} vs $H/t^{\gamma+\beta}$ with the exponent and T_C values from the previous three figures. The different symbols represent different temperatures. While the linear plot—the main body of this figure—makes evident differences in higher fields, the double-logarithmic plot of the inset emphasizes differences in lower fields and also demonstrates the collapse of magnetization isotherms in the critical regime onto the two branches of the scaling function. The solid lines drawn in this inset represent the asymptotic forms of the scaling function discussed in the text.

Complete scaling of all these data in the intervals $242.0 \leqslant T \leqslant 247.5, 200 \leqslant H \leqslant 50\,000$ Oe is demonstrated in Fig. 6 through plots of $M|t|^{-\beta}$ vs $Ht^{-(\gamma+\beta)}$ with the above listed exponent values. This same plot is reproduced on a double-logarithmic scale in the inset in this figure, again convincingly demonstrating scaling of these data onto the two "branches" of the scaling function $(F_+, t>0; F_-, t<0)$. The significance of the solid lines drawn in this inset are next discussed. While the functional form of the scaling functions $F_{\pm}$ are not known in general, the asymptotic behavior at large and small values of the argument $(h/|t|^{\gamma+\beta})$ is established:

$$F_-(0) = M_S(0) \quad (H \to 0,\ T < T_C), \tag{6}$$

$$F_+\left(\frac{h}{t^{\gamma+\beta}}\right) \sim \chi_0 \frac{h}{t^{\gamma+\beta}} \quad (H \to 0,\ T > T_C), \tag{7}$$

$$F_{\pm}(\infty) \sim \left(\frac{1}{D}\frac{h}{t^{\gamma+\beta}}\right)^{1/\delta} \quad (t = 0,\ H > 0), \tag{8}$$

i.e., in Eq. (8) the dependence on reduced temperature is eliminated along the critical isotherm if the Widom equality is satisfied. The latter is certainly satisfied here, with the right-hand side of the equality $\gamma = \beta(\delta - 1)$ yielding a value of 1.394 ± 0.02, which compares very well with the measured γ value listed earlier. The values for $M_S(0), \chi_0$, and D determined from the insets in Figs. 3–5 (and listed in Table I) correspond to these three solid lines; these asymptotic values for the scaling function represent the corresponding data well, further demonstrating a high degree of self-consistency.

TABLE I. Parameters deduced by fitting Eqs. (2)–(4) to the appropriate data. The considerably larger uncertainty in D reflects (Ref. 29) the marked dependence of this parameter on the final choice for T_C and the ensuing value for δ. The uncertainty listed below was estimated by examining isotherms closest to T_C ($\Delta T \leqslant 0.5$ K) and assuming a temperature stability of ± 0.03 K (i.e., $\Delta T/T \sim 10^{-5}$) in addition to the "best fit" uncertainties (± 0.04) in δ found from the critical isotherm itself. This results in a combined uncertainty of ± 0.06 in δ.

$M_S(0)$(emu/g)	χ_0(emu/g Oe)	D(emu/Oe$^{1/\delta}$)
120.8 ± 1.6	$(6.8 \pm 0.2) \times 10^{-5}$	$(1.8 \pm 0.4) \times 10^{-4}$

Having established the exponent values for this system, a number of comparisons appear to be in order. In recent studies of the critical behavior of single-crystal $La_{1-x}Sr_xMnO_3$, Kim *et al.*[9] and Ghosh *et al.*[7] report exponent values ($\gamma = 1.27 \pm 0.06$, $\beta = 0.40 \pm 0.02$, $\delta = 4.12 \pm 0.33$, and $\alpha = 0.05 \pm 0.07$ for $x = 0.25$; $\gamma = 1.22 \pm 0.03$, $\beta = 0.37 \pm 0.04$, $\delta = 4.25 \pm 0.2$ for $x = 0.3$) intermediate between mean-field and three-dimensional Ising model predictions[23] ($\gamma = 1.237, \beta = 0.326, \delta = 4.789, \alpha = 0.11$). With this result in mind we have also carried out a detailed analysis, along the lines summarized above, to investigate the applicability of Ising and *XY* model exponents to single-crystal $La_{0.73}Ba_{0.27}MnO_3$. Given the reasonable proximity of the γ and β values for the Heisenberg and *XY* models[24] ($\gamma = 1.318, \beta = 0.349, \delta = 4.780$), not surprisingly a modified Arrott representation of the present data produces plots with comparable quality to those shown in Fig. 2; indeed, an essentially identical estimate of $T_C = 245.0 \pm 0.5$ K ensues. By contrast to the behavior reported for Heisenberg exponent values, however, the corresponding power-law plots using $M_S(T)$ and $\chi_i(T)$ deduced from such modified Arrott plots are *not* self-consistent. They iterate toward *higher* (i.e., Heisenberg model) exponent values. The situation resulting from the use of Ising exponents is more marked, as expected, as this model predicts exponents further removed from the Heisenberg model. These results provide strong support for our assertion of the applicability of Heisenberg-like behavior for this Ba-substituted system.

While the cubic structure of the Sr-substituted single crystals studied by Kim *et al.*[9] and Ghosh *et al.*[7] might have led to the expectation that they display Heisenberg model exponents,[25] Kim and co-workers argue that the presence of a shape induced uniaxial anisotropy causes a crossover between universality classes. In particular, through measurements (albeit at room temperature) of the easy- (K_E) and hard- (K_H) axis anisotropy constants they estimate that a crossover to three-dimensional Ising model exponents should occur near $t \sim 2 \times 10^{-2}$; furthermore, as the temperature interval over which three-dimensional Heisenberg model exponents are expected to be extracted is very limited, Kim *et al.*[9] argue that a crossover from mean-field to three-dimensional Ising exponents should occur essentially directly, as indeed they report. No such crossover effects have been seen in the present study. Unfortunately no direct means—such as torque magnetometry—is currently available to us, so that

TABLE II. Deduced critical amplitudes in various models for a range of spin values, and the corresponding experimental estimates.

Reduced critical amplitude	Mean field $S=1/2, S=1.87$	fcc Heisenberg $S=1/2, S=\infty$	fcc Ising $S=1/2, S=3/2$	Expt.
$M_S(0)/M_0$	1.73, 1.53	1.69, 1.22–1.44	1.49, 1.31	1.40 ± 0.01
$\mu_{\text{eff}}H_0/k_BT_C$	1.73, 2.99	1.58	1.52	$(0.49\pm0.01)\mu_{\text{eff}}$
$DM_S(0)^{\delta}/H_0$	1.0	1.55, 1.23–2.07	1.88	$1.2^{+0.26}_{-0.04}$

comparisons of the type provided by Kim *et al.*[9] cannot be effected. Notwithstanding this limitation, the dimensions of the sample used in the current experiment should result in any shape induced anisotropy rendering the cylindrical axis as the easy axis. Furthermore, the *lack* of any observed crossover behavior would require the product $K_H\xi^3$ to be at least an order of magnitude smaller than in the corresponding Sr-substituted system (and this, indirectly, would require the product $K_E\xi^3$ to also be smaller, but not necessarily by such a significant amount).

Kim *et al.*[9] also discussed the possible origin of the mean-field-like behavior reported by Mohan *et al.*[8] for polycrystalline $La_{0.8}Sr_{0.2}MnO_3$—likely the result of the correlation length $\xi=\xi_0|t|^{-\nu}$ exceeding the grain size. Previous studies of critical behavior in the $La_{1-x}Ba_xMnO_3$ system have also reported varying results. A polycrystalline specimen with $x=0.33$ yielded $\gamma=1.29$ and $\beta=0.464$ over an undefined (reduced) temperature range,[26] values intermediate between mean-field and three-dimensional Heisenberg model predictions. By contrast, measurements on an epitaxial film[27] with $x=0.3$ yielded mean-field exponents ($\gamma=1.04\pm0.04, \beta=0.54\pm0.02, \delta=3.08\pm0.04$) over a comparable reduced temperature range to that covered in the present investigation. These latter exponent values might possibly arise as a result of a change from Heisenberg to Ising behavior induced by a tetragonal distortion in the film, accompanied by enhanced dipole-dipole interactions[28] (emanating from large spin moments). It is also possible that the correlation length exceeded the film thickness of 150 nm close to T_C causing complications due to reduced dimensionality; a detailed check, however, on this possibility has yet to be made.

Additional evidence supporting the assignment of the universality class of a bulk single crystal (the most appropriate to establish the true critical behavior) to that of the three-dimensional near-neighbor Heisenberg model comes from a consideration of the critical amplitudes. The critical indices (γ, β, and δ) discussed above, while differing between universality classes, do *not* exhibit a dependence on spin values within these classes. By contrast, critical amplitudes display both a model and a spin dependence. In mean-field theory, for example, it is well established that:

$$\frac{M_S(0)}{M_0}=\left\{\frac{10(S+1)^2}{3(2S^2+2S+1)}\right\}^{1/2},$$

M_0 being the zero-temperature saturation magnetization

$$\frac{\mu_{\text{eff}}H_0}{k_BT_C}=\left\{\frac{30S^2}{(2S^2+2S+1)}\right\}^{1/2}$$

where $\chi_0H_0=M_S(0)$ and μ_{eff} is the associated fluctuating moment, while

$$\frac{DM_S(0)^{\delta}}{H_0}=1.$$

Table II lists values for these critical amplitudes for some of the most widely encountered universality classes and a range of spin values.[29] The corresponding experimental values obtained from the data shown in Table I are also shown in this table.

While numerical values for the various critical amplitudes also display a dependence on the lattice structure, we have chosen to list amplitudes deduced for fcc lattices. The principal reason for this choice is the wider range of spin values for which amplitudes have been estimated on this lattice. $La_{1-x}Ba_xMnO_3(x\sim0.3)$ is, however, frequently indexed by a rhombohedral unit cell; the relationship between this and the primitive (pseudocubic) unit cell has been made clear by a number of authors.[30] More importantly, available data[31] indicate that the (pseudo)"cubic" unit cell has dimensions $a=b=3.9120$ Å, some 0.25% larger than $c=3.9001$ Å; indeed it is recognized that among optimally doped ($x=1/3$) manganites $LaAMnO_3$ (A=Ca, Sr, Ba), Ba doping produces the largest mean A site radius[31,32] $\langle r_A\rangle=1.292$ Å with lattice parameters close to those of the ideal cubic structure (as indicated above) and associated Mn-O-Mn bond angle closest to 180°.

A comparison then between the reduced critical amplitudes displayed in Table II for single-crystal $La_{0.73}Ba_{0.27}MnO_3$ and theoretical estimates shows satisfactory agreement with Heisenberg model predictions for the ratio $M_S(0)/M_0$ in the case $S>1/2$, but clear disagreement with mean-field predictions for both $S=1/2$ and $S=3.73/2$ (the average spin value deduced from the low-temperature saturation magnetization). The μ_{eff} value deduced from the experimental amplitude $\mu_{\text{eff}}H_0/k_BT_C$ using the Heisenberg model result (admittedly not completely self-consistent as the model utilizes $S=1/2$) is $\mu_{\text{eff}}=3.22\mu_B$, a difference of some 14% from the experimentally determined saturation moment. Using the "best estimate" for D deduced from the critical isotherm (along with the associated δ estimate) results in the ratio $DM_S(0)^{\delta}/H_0\cong1.2$, significantly higher than the mean-field prediction, but just marginally less than the lowest estimate (1.23) for this ratio for the $S=\infty$, fcc Heisen-

berg model. Moreover, as indicated in the caption to Table I, as D has significant uncertainty associated with it, the upper limit on the ratio in question (1.46) falls well within the range of Heisenberg model predictions for $S>1/2$.

IV. SUMMARY AND CONCLUSIONS

The analysis of detailed measurements of the field and temperature dependent magnetization of a single crystal of $La_{0.73}Ba_{0.27}MnO_3$ reveals the occurrence of a continuous magnetic phase transition at $T_C=245.0\pm0.5$ K. The critical exponents characterizing this transition—estimated self-consistently from modified Arrott plots—are $\gamma=1.39(2)\pm0.005$, $\beta=0.364\pm0.003$, and $\delta=4.83\pm0.04$, very close to those predicted for the three-dimensional near-neighbor Heisenberg model. The critical amplitudes are also in overall agreement with the same model. These results confirm predictions for the universality class of the double-exchange model[25] when anisotropy effects are not important.

ACKNOWLEDGMENTS

This work was supported in part by grants from the Natural Sciences and Engineering Research Council (NSERC) of Canada.

[1] G. H. Jonker and J. H. van Santen, Physica (Amsterdam) **16**, 337 (1950); **16**, 599 (1950); C. W. Searle and S. T. Wang, Can. J. Phys. **47**, 2703 (1969); **48**, 2023 (1970).

[2] A. P. Ramirez, J. Phys.: Condens. Matter **9**, 8171 (1997); T. A. Kaplan and S. D. Mahanti, *Physics of Magnetism* (Plenum, New York, 1999); J. M. D. Coey, M. Viret, and S. von Molnar, Adv. Phys. **48**, 167 (1999); Y. Tokura, *Colossal Magnetoresistive Oxides* (Gordon and Breach, Amsterdam, 2000).

[3] E. Dagotto, T. Hotta, and A. Moreo, Phys. Rep. **344**, 1 (2001).

[4] J. Mesot, P. Allenspach, U. Staub, A. Furrer, and H. Mutka, Phys. Rev. Lett. **70**, 865 (1993); A. Furrer *et al.*, Physica C **235-240**, 261 (1994); J. Liu, J. Wan, A. Goldman, Y. Chang, and P. Jiang, Phys. Rev. Lett. **67**, 2195 (1991); A. Chang, Z. Rong, Y. Ivanchenko, F. Lu, and E. Wolf, Phys. Rev. B **46**, 5692 (1992); T. Cren, D. Roditchev, W. Sacks, and J. Klein, Phys. Rev. Lett. **84**, 147 (2000); K. M. Lang, V. Madhavan, J. E. Hoffman, E. W. Hudson, H. Eisaki, S. Uchida, and J. C. Davis, Nature (London) **415**, 412 (2002).

[5] D. Kim, B. Revaz, B. L. Zink, F. Hellman, J. J. Rhyne, and J. F. Mitchell, Phys. Rev. Lett. **89**, 227202 (2002); J. E. Gordon, C. Marcenat, J. P. Franck, I. Isaac, G. Zang, R. Lortz, C. Meingast, F. Bouqet, R. A. Fisher, and N. E. Phillips, Phys. Rev. B **65**, 024441 (2002).

[6] X. Z. Zhou, H. P. Kunkel, J. H. Zhao, P. A. Stampe, and Gwyn Williams, Phys. Rev. B **56**, R12714 (1997); J. Mira, J. Rivas, F. Rivadulla, C. Vázquez-Vázquez, and M. A. López-Quintela, *ibid.* **60**, 2998 (1999); J. H. Zhao, T. Song, H. P. Kunkel, X. Z. Zhou, R. M. Roshko, and Gwyn Williams, J. Phys.: Condens. Matter **12**, 6903 (2000).

[7] K. Ghosh, C. J. Lobb, R. L. Greene, S. G. Karabashev, D. A. Shulyatev, A. A. Arsenov, and Y. Mukovskii, Phys. Rev. Lett. **81**, 4740 (1998).

[8] Ch. V. Mohan, M. Seeger, H. Kronmüller, P. Murugaraj, and J. Maier, J. Magn. Magn. Mater. **183**, 348 (1998)); M. C. Martin, G. Shirane, Y. Endoh, K. Hirota, Y. Moritomo, and Y. Tokura, Phys. Rev. B **53**, 14285 (1996); P. Lin, S. H. Chun, M. B. Salamon, Y. Tomioka, and Y. Tokura, J. Appl. Phys. **87**, 5825 (2000).

[9] D. Kim, B. L. Zink, F. Hellman, and J. M. D. Coey, Phys. Rev. B **65**, 214424 (2002)

[10] A. Moreo, M. Mayr, A. Feiguin, S. Yunoki, and E. Dagotto, Phys. Rev. Lett. **84**, 5568 (2000); J. Burgy, M. Mayr, V. Martin-Mayor, A. Moreo, and E. Dagotto, *ibid.* **87**, 277202 (2001).

[11] A. S. Alexandrov and A. M. Bratkovsky, Phys. Rev. Lett. **82**, 141 (1998); J. Phys.: Condens. Matter **11**, 1989 (1999); **11**, L531 (1999).

[12] A. J. Millis, P. B. Littlewood, and B. I. Shraiman, Phys. Rev. Lett. **74**, 5144 (1995); A. J. Millis, B. I. Shraiman and R. Mueller, *ibid.* **77**, 175 (1996); Q. Li, J. Zhang, A. R. Bishop, and C. M. Soukoulis, Phys. Rev. B **56**, 4541 (1997); S. Murakami and N. Nagaosa, Phys. Rev. Lett. **90**, 197201 (2003).

[13] A. Urushibara, Y. Moritomo, T. Arima, A. Asamitsu, G. Kido, and Y. Tokura, Phys. Rev. B **51**, 14103 (1995)

[14] Y. Tomioka, A. Asamitsu, H. Kuwahara, Y. Moritomo, and Y. Tokura, Phys. Rev. B **53**, R1689 (1996)

[15] H. L. Ju, J. Gopalakrishnan, J. L. Peng, Qi Li, G. C. Xiong, T. Venkatesan, and R. L. Greene, Phys. Rev. B **51**, 6143 (1995); R. Von Helmolt, J. Wecker, B. Holzapfel, L. Schultz, and K. Samwer, Phys. Rev. Lett. **71**, 2331 (1993)

[16] D. Shulyatev, S. Karabashev, A. Arsenov, and Y. Mukovskii, J. Cryst. Growth **199**, 511 (1999).

[17] P. A. Stampe and G. Williams, J. Phys.: Condens. Matter **10**, 6771 (1998); Z. Wang, H. P. Kunkel, and G. Williams, *ibid.* **2**, 4173 (1990).

[18] J. A. Osborn, Phys. Rev. **67**, 351 (1945).

[19] S. K. Banerjee, Phys. Lett. **12**, 16 (1964); J. Mira *et al.*, Ref. 6; N. Moutis, I. Panagiotopoulos, M. Pissas, and D. Niarchos, Phys. Rev. B **59**, 1129 (1999).

[20] H. E. Stanley, *Introduction to Phase Transitions and Critical Phenomena* (Clarendon, Oxford, 1971).

[21] A. Arrott and J. E. Noakes, Phys. Rev. Lett. **14**, 786 (1967).

[22] M. Campostrini, M. Hasenbusch, A. Pelissetto, P. Rossi, and E. Vicari, Phys. Rev. B **65**, 144520 (2002).

[23] Massimo Campostrini, Andrea Pelissetto, Paolo Rossi, and Ettore Vicari, Phys. Rev. E **60**, 3526 (1999).

[24] Massimo Campostrini, Martin Hasenbusch, Andrea Pelissetto, Paolo Rossi and Ettore Vicari, Phys. Rev. B **63**, 214503 (2002).

[25] J. L. Alonso, L. A. Fernández, F. Guinea, V. Laliena, and V. Martin-Mayor, Nucl. Phys. B **596**, 587 (2001); Y. Motome and N. Furukawa, J. Phys. Soc. Jpn. **68**, 3853 (1999); **69**, 3785 (2000); **70**, 1487 (2001).

[26] N. Moutis *et al.*, Ref. 19.

[27] M. Ziese, J. Phys.: Condens. Matter **13**, 2919 (2001).

[28] A. Aharony, Phys. Rev. B **8**, 3363 (1973); M. E. Fisher and A. Aharony, Phys. Rev. Lett. **30**, 559 (1973); A. Aharony and M. E. Fisher, Phys. Rev. B **8**, 3323 (1973).

[29] S. Milosevic and H. E. Stanley, Phys. Rev. B **6**, 986 (1972); **6**, 1002 (1972); R. Krasnow and H. E. Stanley, *ibid.* **8**, 332 (1973); C. Domb and M. S. Green, *Phase Transitions and Critical Phenomena* (Academic, New York, 1974); S. N. Kaul, J. Magn. Magn. Mater. **53**, 5 (1985).

[30] J. B. Goodenough and P. M. Raccah, Phys. Rev. **155**, 932 (1967); J. F. Lawler, J. M. D. Coey, J. G. Lunney, and V. Skumryev, J. Phys.: Condens. Matter **8**, 10737 (1996).

[31] N. Moutis *et al.*, Ref. 19, Table 1; A. B. Beznosov, V. A. Desnenko, E. L. Fertman, C. Ritter, and D. D. Khalyavin, Phys. Rev. B **68**, 054109 (2003) deduce room temperature values $a = b = 3.9165$ Å, also about 0.25% larger than $c = 3.9061$ Å.

[32] P. G. Radaelli, G. Iannone, M. Marezio, H. Y. Hwang, S-W. Cheong, J. D. Jorgensen, and D. N. Argyriou, Phys. Rev. B **56**, 8265 (1997).